JOURNAL OF AGRICULTURAL AND FOOD CHEMISTRY

Usefulness of Fluorescence Excitation−Emission Matrices in Combination with PARAFAC, as Fingerprints of Red Wines

DIEGO AIRADO-RODRÍGUEZ,*,† TERESA GALEANO-DÍAZ,† ISABEL DURÁN-MERÁS,† AND JENS PETTER WOLD§

Nofima Mat AS, Norwegian Food Research Institute, Osloveien 1, N-1430 Aas, Norway, and Department of Analytical Chemistry, University of Extremadura, Avenida de Elvas s/n, 06071 Badajoz, Spain

The possibility of using front-face fluorescence spectroscopy to characterize red wines was investigated, and a tentative identification of their main fluorescent components was attempted. Fifty-seven red wine samples from different origins were included in the present study. Their fluorescence excitation−emission matrices (EEMs) were registered directly on 3-mL aliquots of untreated samples. The assayed excitation and emission ranges were 245−340 and 300−500 nm, respectively. The set of 57 EEMs was analyzed by means of parallel factor analysis (PARAFAC). Thus, the spectral excitation and emission profiles of possible "pure" fluorescence components (PARAFAC loadings) and the relative contribution of each component to the individual EEMs (PARAFAC scores) were obtained. The red wine system contained four main fluorescence components, and the excitation and emission loadings had maxima at the wavelength pairs 260/380, 275/323, 330/410, and 280/364 nm, respectively. A tentative identification of fluorophores was done by matching PARAFAC score values with HPLC measurements on the same 57 samples, as well as fluorescence measurements on pure compounds typically present in red wine. It was found that the third component was highly correlated with concentrations of catechin and epicatechin. When the PARAFAC score values were plotted against each other, they did to some extent discriminate the wines according to origin (country) and grape variety.

KEYWORDS: Wine; polyphenols; front-face fluorescence; excitation−emision matrices; parallel factor analysis

INTRODUCTION

The interest in studying the chemical composition of wine is prompted by its importance for assessing wine quality. It is important to develop fast analytical methods without sample pretreatment. During recent years, customers have been raising their demands for the quality of wine, and the quality has correspondingly been improved by the wine industry. There is a growing need for efficient tools to handle and address the chemical analysis of wines in order to automate the production and stabilize the quality. Tools that allow classification of wine depending on the region of origin, grape variety, or winemaking process can be helpful for this industry. Fast tools for detection of fraud in the wine industry would be helpful.

Three-dimensional fluorescence spectroscopy has proven to be very useful for nondestructive analysis of complex food matrices, for either authenticity, quality classification, or detailed chemical characterization (*1*). The technique involves successive acquisition of excitation or emission spectra at multiple emission or excitation wavelengths, respectively. The resulting emission−excitation data matrix (EEM) provides a total intensity profile of the sample over the range of scanned excitation and emission wavelengths. This technique is fast, noninvasive, sensitive, and relatively low-cost. Fluorescence spectroscopy can provide information about fluorescent molecules and their environment in biological and food samples and is reported to be 100−1000 times more sensitive than spectrophotometric techniques (*2*).

Conventional right-angle fluorescence is the most common optical setup used for transparent and diluted solutions. Front-face fluorescence, however, can be recorded directly on the surface of turbid or solid intact samples. The front-face illumination angle may vary between 30° and 60°. Thus, fluorophores such as riboflavin, chlorophyll, tryptophan, tyrosin, phenylalanine, NADH, collagenous connective tissue, and

* Address correspondence to this author at Departamento de Química Analítica, Universidad de Extremadura, Avda. de Elvas s/n, 06071 Badajoz, Spain (telephone +34 924289375; fax +34 924274244; e-mail airado@unex.es).

† University of Extremadura.

§ Nofima Mat AS (Norwegian Food Research Institute).

10.1021/jf8033623 CCC: $40.75
Published on Web 02/12/2009

Table 1. Origin and Grape Variety in Analyzed Wine Samples

sample	origin	code	grape variety
1	France	F1	Cabernet Sauvignon
2	France	F2	
3	Chile	Ch3	Cabernet Sauvignon
4	Chile	Ch4	Cabernet Sauvignon
5	Chile	Ch5	Cabernet Sauvignon
6	Chile	Ch6	Cabernet Sauvignon
7	Chile	Ch7	Cabernet Sauvignon
8	Chile	Ch8	Cabernet Sauvignon
9	Chile	Ch9	Merlot
10	Chile	Ch10	Cabernet Sauvignon
11	Chile	Ch11	Cabernet Sauvignon
12	Chile	Ch12	Cabernet Sauvignon
13	Chile	Ch13	
14	Chile	Ch14	
15	South Africa	S-Af15	Cabernet Sauvignon
16	South Africa	S-Af16	Cabernet Sauvignon
17	South Africa	S-Af17	Cabernet Sauvignon
18	Australia (Western)	W-A18	Shiraz
19	Australia (Western)	W-A19	Shiraz
20	Australia	A20	Shiraz, Cabernet Sauvignon
21	Australia	A21	Shiraz, Cabernet Sauvignon
22	Australia	A22	
23	Australia	A23	
24	Spain	S24	
25	Spain	S25	
26	Spain	S26	
27	Argentina	Ar27	Malbec, Syrah, Bonarda
28	Argentina	Ar28	Malbec, Syrah, Bonarda
29	Argentina	Ar29	Malbec, Syrah, Bonarda
30	Argentina	Ar30	Syrah
31	Argentina	Ar31	Syrah
32	Argentina	Ar32	Syrah
33	United States	USA33	Syrah
34	United States	USA34	Ruby Cabernet
35	United States	USA35	Ruby Cabernet
36	Italy	I36	
37	Italy	I37	
38	Italy (Sicily)	I38	
39	Italy	I39	Sangiovese
40	Italy	I40	Sangiovese
41	Italy	I41	
42	Italy	I42	
43	Italy	I43	
44	Tunisia	T44	
45	Italy	I45	
46	Italy	I46	
47	Italy	I47	
48	Italy	I48	
49	Italy	I49	
50	Italy	I50	
51	Chile	Ch51	
52	Chile	Ch52	
53	Chile	Ch53	Merlot
54	Chile	Ch54	Merlot
55	Portugal	P55	
56	Portugal	P56	
57	Italy	I57	Sangiovese

various oxidation products can be detected and quantified nondestructively (*1*).

Dufour and co-workers (*3*) have previously investigated the usefulness of single excitation (250−350 nm, λ_{em} 376 nm) and emission (275−450 nm, λ_{exc} 261 nm) spectra of wines for the purpose of distinguishing the variety, typicality, and vintage of French and German wines. Emission spectra were characterized by a maximum at 376 nm, with a shoulder at 315 nm. The most important marker was found to be the intensity ratio between peak and shoulder. This preliminary study showed that front-face fluorescence spectroscopy combined with chemometrics offers a promising approach for the authentification of wines.

Table 2. Fluorescent Properties of Assayed Fluorescent Molecules, in 3 g/L Tartrate Buffer at pH 3.7 and Ethanol 13% v, and Four PARAFAC Components

		compound	λ_{exc} (nm)	λ_{em} (nm)
non-flavonoids	phenolic acids	gallic acid	241	350
		p-coumaric acid	348	410
		vanillic acid	241, 282, 305	354
		caffeic acid	262	433
		ellagic acid	333	422
		sinapic acid	297, 335	446
		ferulic acid		
		gentisic acid	320	446
	stilbenes	*trans*-resveratrol	318	390
		trans-piceid	318	390
flavonoids	flavonols	quercetin	427	480
		rutin		
	flavanols	catechin	279	317
		epicatechin	280	316
	anthocyanins	malvidin-3-*O*-β-glucopyranoside	280	355
		delphinidin-3-*O*-β-glucopyranoside	280	355
		petunidin-3-*O*-β-glucopyranoside	280	355
	PARAFAC component 1		260	380
	PARAFAC component 2		275	323
	PARAFAC component 3		330	410
	PARAFAC component 4		260, 280	364

Bilinear models have been successfully applied to evaluate data sets of single autofluorescence spectra of meat (*4*), fish (*5*), dairy products (*6*), cereals (*7*), fruit juices (*8*), and honey (*9*). A set of EEMs follows the three-way parallel factor analysis (PARAFAC) decomposition model (*10*, *11*) and can thus be decomposed into scores, emission and excitation loadings, enabling a more thorough interpretation of the system. Such multiway models have been applied to autofluorescence landscapes of intact food systems (*1*), such as sugar (*12*), meat (*13*), fish oil (*14*), yogurt (*15*), cheese (*16*), and edible oils (*17*, *18*). No references to the usefulness of fluorescence landscapes of wines have been found.

In the present paper, excitation−emission fluorescence matrices of red wines are presented and analyzed. The main aim of this work was to detect the main fluorescent components in red wine and assign them to possible fluorescent compounds. This was done by the use of a PARAFAC model applied on fluorescence landscapes of different wine samples. A wide variety of red wine samples from different origins were collected in order to span variation in quality and fluorescence properties, EEMs were recorded from each wine, and a PARAFAC model was developed. A tentative identification of the fluorophores in wine was done by matching the PARAFAC scores from each sample with HPLC measurements on the same samples and fluorescence measurements on pure compounds. As wines from different countries were included in the PARAFAC model, the capability of discriminating between origins was elucidated. The influence of the grape variety on the fluorescent properties was also studied.

MATERIALS AND METHODS

Wine Samples. Fifty-seven red wines from different origins were included in this study: 2 samples from France, 16 from Chile, 3 from

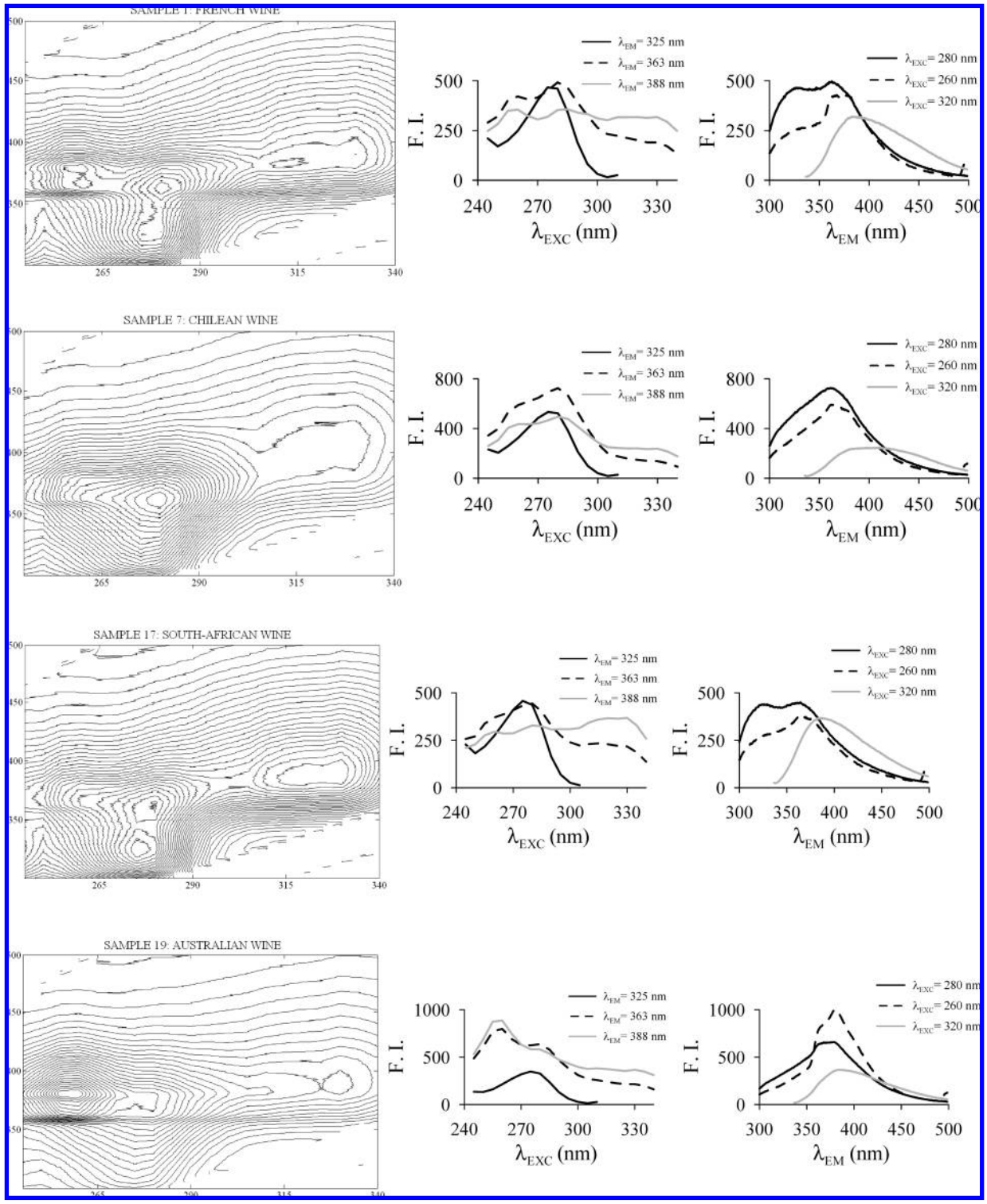

Figure 1. (Left) Fluorescence landscapes (as contour plots) corresponding to wine samples 1 (French), 7 (Chilean), 17 (South African), and 19 (Australian). (Middle) Extracted excitation spectra. (Right) Extracted emission spectra.

South Africa, 6 from Australia (2 of them from the Western zone), 3 from Spain, 6 from Argentina, 3 from the United States, 15 from Italy, 1 from Tunisia, and 2 from Portugal (**Table 1**). A code was assigned to each sample, indicating country of origin and sample number (**Table 1**). Grape variety is also listed in **Table 1** when known. Samples were stored at 4 °C. Prior to the measurements, samples were equilibrated at 15 °C. The EEM was registered immediately after each bottle was opened.

Fluorescence Spectroscopy. Fluorescence measurements were collected with a Perkin-Elmer LS50B fluorescence spectrophotometer equipped with a variable-angle front-face accessory, to ensure that reflected light, scattered radiation, and depolarization phenomena were minimized. The angle of incidence, defined as the angle between the excitation beam and a perpendicular to the cell surface, was 30°. Wine samples were placed in a 3 mL quartz cell, and spectra were recorded at 15 °C. Slits at excitation and emission monochromators were set at 15 and 5 nm, respectively. Acquisition speed was fixed at 500 nm/min, as a compromising solution between noise in the spectra and collection time. Excitation and emission wavelength ranges were 245−340 and 300−498.5 nm, respectively, with wavelength increments of 5 and 0.5 nm, respectively. The landscapes were registered as multiple emission spectra at decreasing excitation wavelengths, starting at 340 nm and finishing at 245 nm, to avoid sample alteration by the UV excitation beam. Total scanning time per sample was approximately

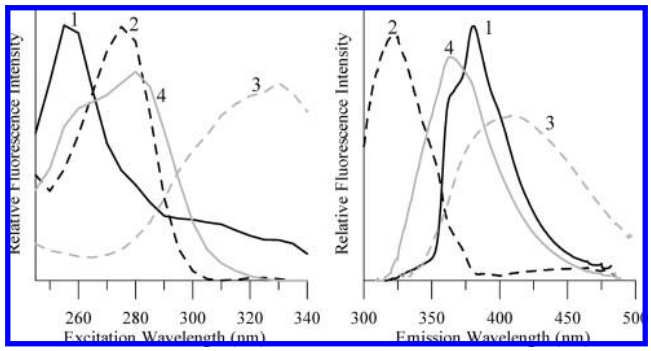

Figure 2. PARAFAC fluorescent loadings for the four components of the non-negativity constrained PARAFAC model constructed on the basis of the fluorescent landscapes of 57 wine samples.

10 min. Measurements were performed within a short period of time (6 days) to minimize the effect of instrumental fluctuation (e.g., lamp intensity).

Fluorescence Measurements on Standards. All chemicals were of analytical grade. Ultrapure water, obtained from a Millipore Milli-Q System, was used throughout. Gallic acid, *p*-coumaric acid, ellagic acid, ferulic acid, gentisic acid, *trans*-resveratrol, *trans*-piceid, quercetin, rutin, catechin, and epicatechin were obtained from Sigma. Vanillic acid, caffeic acid, and sinapic acid were obtained from Fluka. Stock solutions of standards, containing 100 mg/L of each, were prepared in ethanol. Diluted solutions were prepared in a synthetic wine matrix, containing 3 g/L of tartrate buffer at pH 3.7, and 13% v of ethanol. The following procedure was used to collect the spectra: 3 mL of the synthetic wine matrix was added into the quartz cell, and successive small volumes, on the order of microliters, of stock solutions of standards were added. A spectrum was registered after each addition, and the procedure was repeated until we obtained a well-defined spectrum. Instrumental settings were similar to those for wine, but measurements were carried out in the 90° geometry, as all solutions were transparent.

HPLC Analysis. The 57 samples were chromatographed, and the eluates were fluorometrically monitored at the excitation/emission wavelengths pairs corresponding to the obtained PARAFAC components. An appropriate gradient program was chosen to carry out the elution of samples, with the objective of getting a good separation and a good profile of the fluorescent compounds in wine at each specific excitation/emission pair. Thus, three injections were made of each sample, monitoring the eluate at $\lambda_{exc/em}$ 260/360 (compromising wavelengths for obtained PARAFAC components 1 and 4), 275/320 (PARAFAC component 2), and 330/410 nm (PARAFAC component 3), respectively.

Chromatographic Separation. Two-milliliter aliquots of each sample were diluted to a final volume of 10 mL with a mixture of methanol/water 50:50 (v/v). The diluted wine samples were filtered through a Millex FG 0.20 μm filter (Millipore Corp.) before injection (10 μL). Chromatographic separation was performed on a Betasil C18 column (250 mm × 2.1 mm i.d., 5 μm particle size) from Thermo Hypersil-Keystone (Bellefonte PA). Column temperature was 15 °C. The mobile phases were (A) methanol/formic acid/water (10:2:88, v/v) and (B) methanol/formic acid/water (90:2:8, v/v). The gradient used was as follows: 0 min, 100% A; 15 min, 85% A, 15% B; 25 min, 50% A, 50% B; 34 min, 30% A, 70% B. The flow rate was set at 0.25 mL min^{-1}. The column was allowed to equilibrate for 10 min between injections.

All solvents were of gradient grade for liquid chromatography (Merck). All other chemicals were of analytical reagent grade and used without further purification. Ultrapure water, obtained from a Millipore Milli-Q System, was used throughout.

HPLC with DAD and Fluorescence Detection. HPLC analyses were performed using an HP 1050 series HPLC (Hewlett-Packard GmbH, Waldbronn, Germany), equipped with a diode array detector (DAD) scanning from 200 to 600 nm and interfaced to a Shimadzu spectrofluorometric detector model RF-551 (Bergman AS, Lillestrøm, Norway) through an HP-35900 interface.

HPLC with DAD and MS Detection. The analyses were performed on an Agilent 1100 series HPLC system (Agilent Technologies, Waldbronn, Germany) equipped with an autosampler cooled to 6 °C, a DAD scanning from 200 to 600 nm, and an MSD XCT ion trap mass spectrometer with an ESI interface. The LC eluate was introduced directly into the ESI interface without splitting. The interesting compounds were analyzed in negative and positive ion modes. The nebulizer pressure was 40 psi; dry gas flow, 10 L/min; dry temperature,

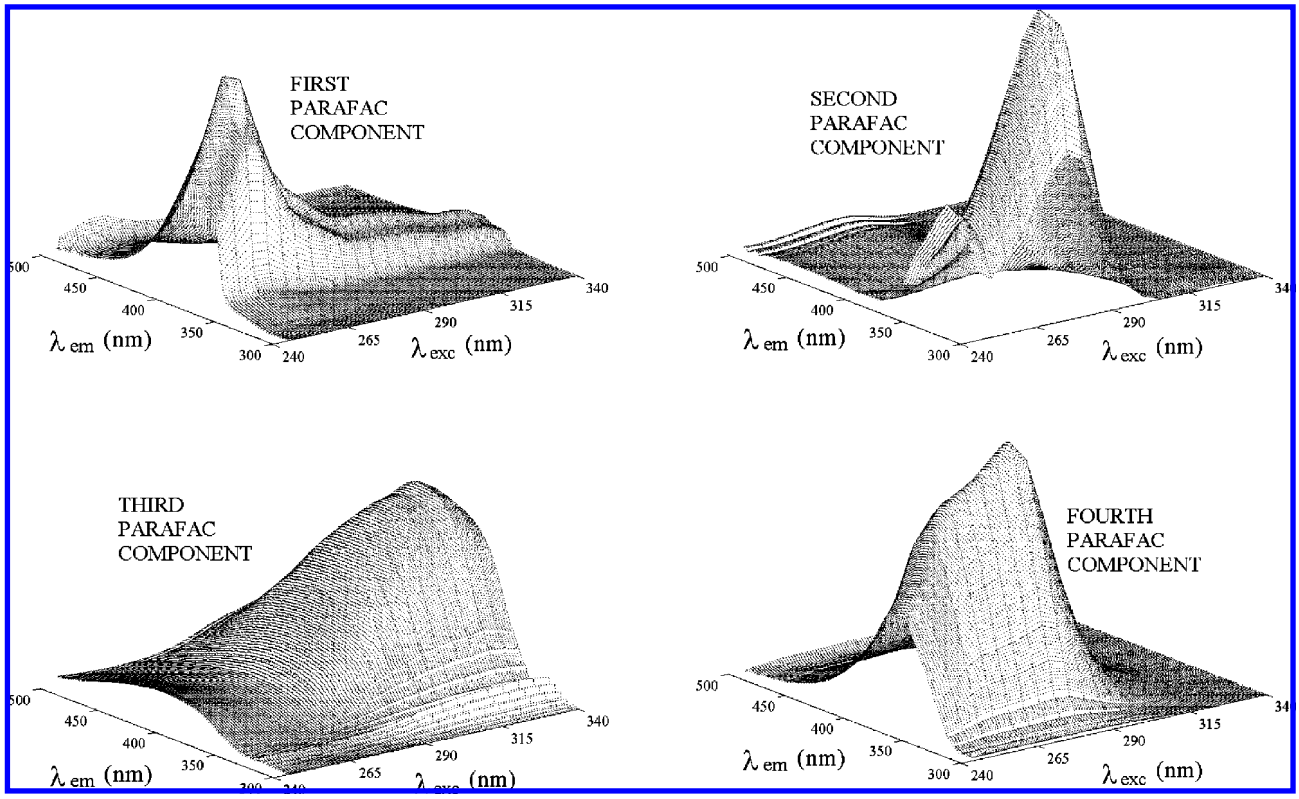

Figure 3. 3D structure of the four PARAFAC components obtained by multiplying the corresponding loading vectors.

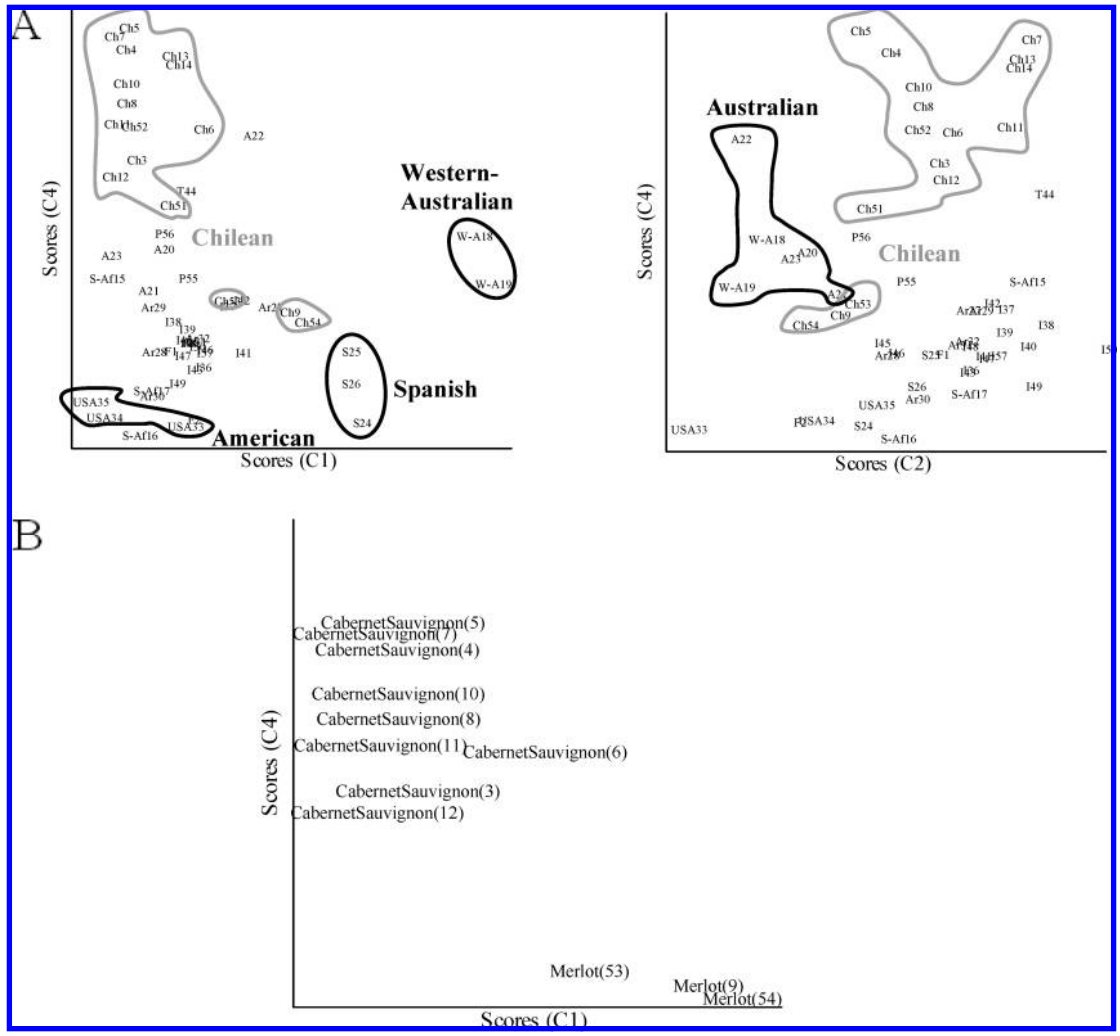

Figure 4. 2D representations of PARAFAC scores corresponding to the fourth component against those corresponding to the first and second ones. Samples are represented according to the origin (**A**) and grape variety within Chilean samples (**B**). Samples in **A** are represented by the codes in **Table 1**.

350 °C; and capillary voltage, 3.5 kV. Analysis was carried out using scan from *m*/*z* 100 to 2200, with a scan speed 27000 amu/s.

Data Modeling. *Pretreatment of Data Set.* Rayleigh signals in all of the EEMs were removed by setting these elements to missing values. Zeros were inserted in the zones where $\lambda_{em} < \lambda_{exc}$, because there is no emission at wavelengths below the excitation wavelength. Zeros instead of missing values in this zone speed the calculations; however, setting zeros close to the identity line can give bias in the solution (*11*). This problem was handled by inserting missing values for a band of emission wavelengths below excitation and zeros for all other emissions below excitation. The bandwidth of missing values was estimated through visual inspection of the data (*19*).

PARAFAC Analysis. When a sample produces a $J \times K$ matrix (a second-order tensor), such as an EEM (J = number of emission wavelengths, K = number of excitation wavelengths), the corresponding set obtained by "stacking" all of the registered matrices is a three-way array. Appropriate dimensions of such a box are $I \times J \times K$ (I = number of samples). As EEMs follow a trilinear model, the three-way array can be written as a sum of tensor product of three vectors for each fluorescent component. If A_n, B_n, and C_n collect the relative concentration ($I \times 1$), emission ($J \times 1$), and excitation ($K \times 1$) profiles for component n, respectively, the data cube $\underline{\mathbf{F}}$ can be written (*20*, *21*)

$$\underline{\mathbf{F}} = \sum_{n=1}^{N} \mathbf{A}_n \otimes \mathbf{B}_n \otimes \mathbf{C}_n + \underline{\mathbf{E}}$$

where $\otimes$ indicates the tensor product, N is the total number of fluorescent components, and $\underline{\mathbf{E}}$ is a residual error term of the same dimensions as $\underline{\mathbf{F}}$. The column vectors $\mathbf{A}_n$, $\mathbf{B}_n$, and $\mathbf{C}_n$ are usually collected into the three loading matrices **A**, **B**, and **C**.

A characteristic property of $\underline{\mathbf{F}}$ is that it can be uniquely decomposed, providing access to spectral profiles (**B** and **C**) and relative concentrations (**A**) of individual components in the I mixtures, whether they are chemically known or not. This constitutes the basis of the so-called second-order advantage ("second-order" refers to the tensor order of a single sample data matrix, in contrast to "third-order", as referred to the cube formed by the matrices of I samples).

The PARAFAC analysis was performed in Matlab ver. 7.1.0 (The Mathworks Inc., Natick, MA) by use of the PLS_Toolbox (Eigenvector Research Inc., Wenatchee, WA).

To model the set of fluorescence data, the EEMs of the 57 samples were arranged in a three-dimensional structure of size 57 × 398 × 20 (samples × number of emission wavelengths × number of excitation wavelengths). This array was decomposed by PARAFAC using different number of components. In all cases, non-negative constraints for the resolved profiles for all modes were applied. This was done to obtain a realistic solution, because concentrations and spectral values are positive.

The Unscrambler software package (*22*) was employed to investigate correlations between PARAFAC scores and chromatographic results.

RESULTS AND DISCUSSION

Excitation−Emission Matrices of Red Wines. Typical EEMs corresponding to four of the analyzed wines samples are shown in **Figure 1** in the form of landscapes. In the same figure

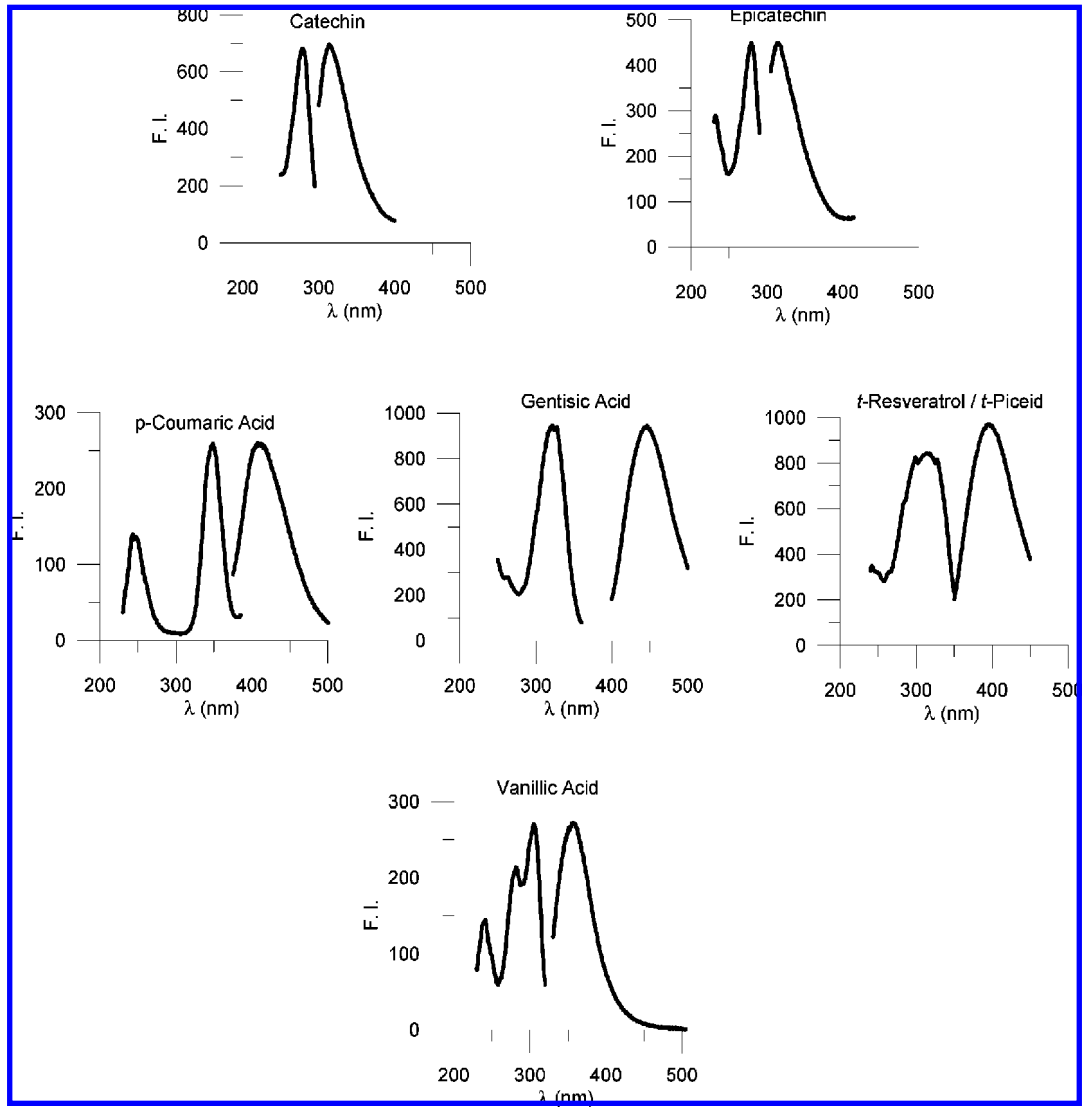

Figure 5. Excitation and emission spectra of some of the assayed standards in 3 g/L tartrate buffer at pH 3.7 and ethanol 13% v.

are also shown the emission and excitation spectra, extracted from these matrices, as vertical and horizontal cuts, respectively, at the wavelengths specified in the figure caption. All samples fluoresce in the emission region between 300 and 400 nm, when they are excited at wavelengths below 290 nm. The excitation (250−350 nm, λ_{em} 376 nm) and emission (275−450 nm, λ_{exc} 261 nm) spectra previously published by Dufour et al. (*3*) for discrimination of French and German wines belong to this spectral region. This region is rather complex, due to several overlapping spectral bands, and it is difficult to analyze and interpret by using single pairs of excitation and emission spectra only. Another fluorescent region was found in the emission zone around 350 and 450 nm, when the sample is excited at wavelengths longer than 290 nm. In the emission spectra at an excitation wavelength of 260 nm, a wide band centered to 372 nm was observed, in which two maxima can be distinguished at 363 and 380 nm. The intensity ratio for these two maxima varied between samples, as previously described by Dufour et al. (*3*). Thus, for example, in sample 19, the fluorescence intensity at 380 nm was higher than at 363, unlike in samples 7 and 17, or in sample 1, in which the intensity ratio was close to 1. Regarding the excitation spectra obtained at 363 nm, two excitation maxima were located at 260 and 280 nm. The relative intensities of these two peaks varied with the samples, like the emission did, for example, the ratio FI (260 nm)/FI (280 nm) being higher than 1 for sample 19 and smaller than 1 for sample 1; also, in other cases, as in samples 7 and 17, the maximum excitation was centered at 280 nm and a simple shoulder was observed at 260 nm.

Interesting emission spectra were obtained at an excitation wavelength of 280 nm. In this case the most intense fluorescent emission was reached around 363 nm, but in some cases, as, for example, in samples 1 and 17, a second maximum was observed around 325 nm. Furthermore, a single excitation maximum at 275 nm was observed at $\lambda_{em} = 325$ nm, being the shape of this spectra independent of the sample.

Lastly, a third prominent and broad emission feature was observed at emission wavelengths around 388 nm. A wide emission maximum was obtained in this case, centered at 388 nm. An excitation maximum was observed at 325 nm for emission wavelength fixed at 388 nm, the shape of these excitation spectra at wavelengths below 300 nm being similar to the one obtained at $\lambda_{em} = 363$ nm.

PARAFAC Results. The excitation and emission profiles of the main variation components were extracted from the set of fluorescent landscapes by applying PARAFAC. Choosing the appropriate number of components was the first step for constructing the PARAFAC model, and this decision was made on the basis of different criteria (*11*), among them, the so-called core consistency diagnostic. Core consistency percentages of

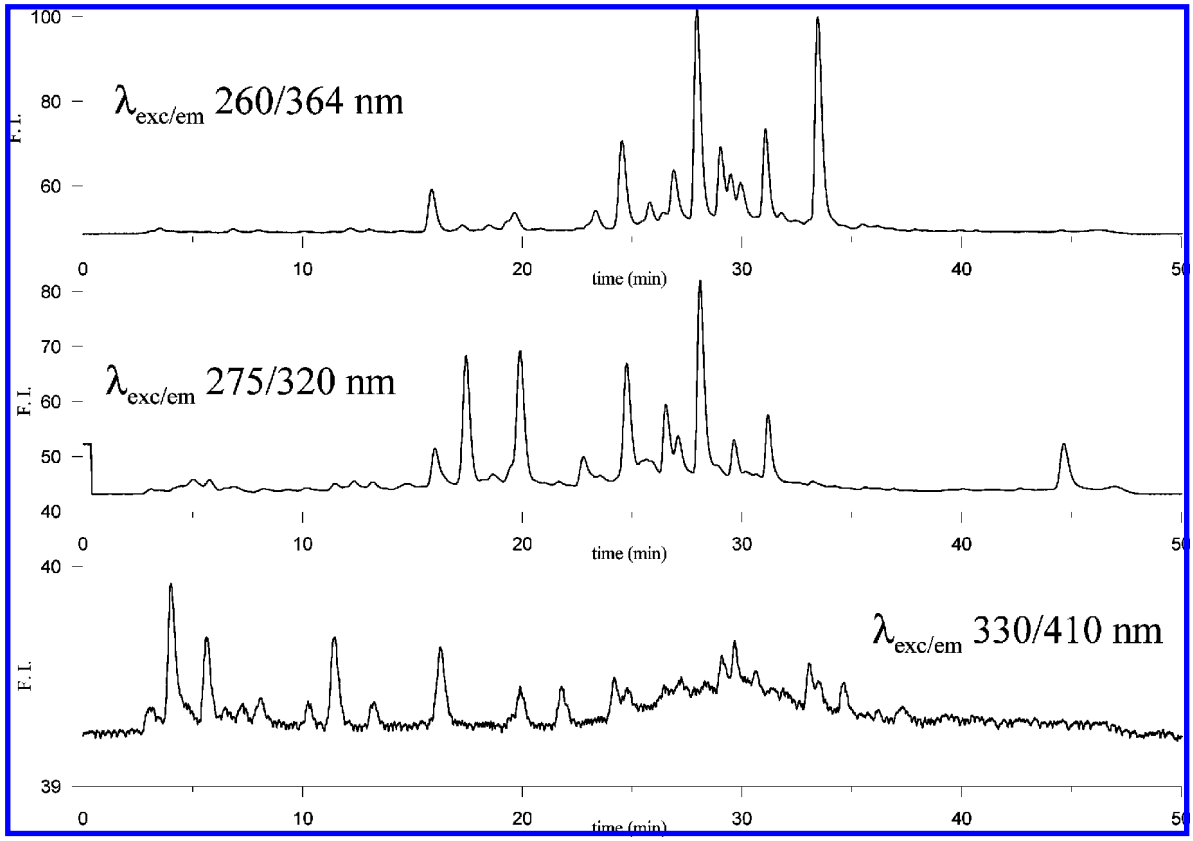

Figure 6. FLD profiles at $\lambda_{exc/em}$ 260/360 (top), 275/320 (middle), and 330/410 nm (bottom), corresponding to the same sample eluted under specified gradient conditions.

100 and 99.7% were calculated for one and two components, respectively, and 50.9, 40.4, and −3.3% for the three-, four-, and five-component models, respectively. It was clear that five components were excessive. The visual appearance of the loadings was helpful and important to finally decide that the optimal number of components in the present case was four. It was observed that in the five-component model, the fifth component was a combination of the first and the fourth, whereas in the four-component model, all of the excitation and emission profiles seemed to be independent from each other.

The stability and uniqueness of the model was tested by split-half analysis (*23*). Thus, different subsets of data were extracted according to several split criteria (even−odd, Italian−non-Italian, and Chilean−non-Chilean samples), and each of them was independently analyzed. The same spectral profiles were obtained in all cases, demonstrating the validity of the constructed model.

The results from the PARAFAC model are shown in **Figures 2** and **3**, in the form of PARAFAC loadings in excitation and emission modes and 3D structures of the PARAFAC components, respectively.

The first-component excitation profile has a narrow maximum centered around 260 nm and a sharp emission maximum at 380 nm, with a shoulder at 365 nm. The pair of excitation/emission wavelengths corresponding to the maximum fluorescent intensity for the second component is 275/323. The third component is a broad peak centered at 330 and 410 nm, respectively. Finally, the fourth component is situated close to the first and second ones, with its excitation profile centered at 280 nm with a shoulder at 260, and the emission one centered at 364 nm.

In addition to the loadings, PARAFAC also provides a score matrix, which represents the contribution of each of the components in the different EEMs contained in the data set. Thus, according to $\underline{\mathbf{F}} = \sum_{n=1}^{N} \mathbf{A}_n \otimes \mathbf{B}_n \otimes \mathbf{C}_n + \underline{\mathbf{E}}$, each EEM can be reconstructed by summing the products of each component's profile by its score value.

Explorative Study of the Score Values. The score values corresponding to each PARAFAC component were plotted against each other in order to study possible systematic information contained in fluorescence data with respect to the known variables origin and grape variety. Some clustering was observed when scores for the fourth PARAFAC component were plotted versus those of the first and second components (**Figure 4A**). In the fourth versus the first PARAFAC score plot, samples 18 and 19 from Western Australia are situated apart from the rest of samples, because these samples had the highest score values in component 1. Spanish samples also had high score values in this component and low values in the fourth component. American samples are characterized by the lowest values of scores in both components, which make these two groups of samples different from the rest. Thirteen of the 16 Chilean samples (except for samples 9, 53, and 54) are clustered in the top side of the graph. An Australian cluster is observed in the score plot for components 4 and 2 apart from the above-described cluster of Chilean samples.

Scores corresponding to the fourth and second PARAFAC components also reveal that a cluster of the Chilean samples are grouped in the top half of the graph, except samples 9, 53, and 54.

Nevertheless, the fact that not all samples are included in clusters according to origin is natural, because this is certainly not the only factor affecting the fluorescent properties of wine samples. Fluorescent compounds of wine (mainly polyphenolic compounds) are mostly generated in the grape pulp, seeds, and skins, and they are partially extracted into wine in the wine-making process; therefore, the variety of grapes would be

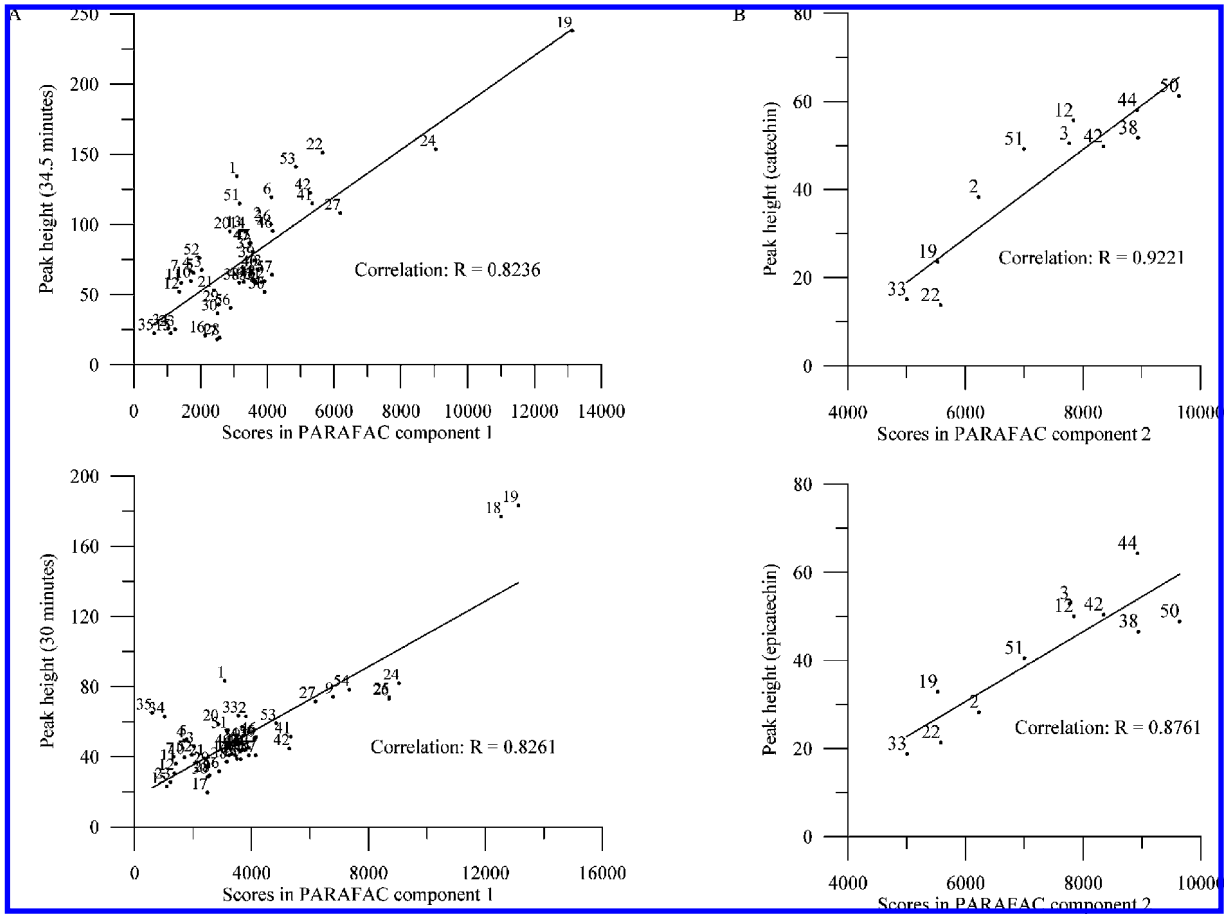

Figure 7. Correlations between score values and single peaks in the chromatograms.

assumed to influence their relative amounts. The environmental conditions in which grapes have been grown, the treatment of the vineyard (e.g., irrigation and pruning), the ripeness of the fruit in the vintage moment, the fermentation techniques employed in the winemaking, the maceration process, and the aging of wine in barrels, among others, are factors that might affect the polyphenolic content and profile (*24*) and, thus, the fluorescent properties of wine.

The effect of grape variety can be observed in the group of Chilean samples. This variable separates samples 9, 53, and 54 from the rest of the samples from the same origin, as these samples are made with Merlot grapes and the rest of the Chilean samples are made from Cabernet Sauvignon grapes. This effect is clearly observed in **Figure 4B**, in which Chilean samples have been extracted from the graph of PARAFAC component 1 against 4, and grape variety is indicated for each one of them.

Although the number of samples is low, the clusters suggest that the fluorescence data contain systematic information related to important quality features of the wines.

Identification of Fluorophores. *Fluorescence of Typical Fluorescent Compounds Present in Wine.* Fluorescent properties of compounds present in wines are highly dependent on the working medium, being influenced by variables such as the acidity or the composition of the medium. It is known that fluorescent behavior is highly affected by the pH and sometimes by the content of organic solvents such as ethanol. Thus, a chemical environment similar to wine matrix has been looked for, and fluorescent measurements of pure compounds were therefore in all cases made in a synthetic wine matrix, containing 3 g/L of tartrate buffer at pH 3.7 and 13% v of ethanol. With regard to the concentration of fluorophores, it is important to highlight that no changes in the position and shape of excitation and emission maxima were observed in the assayed concentration range for any of them, varying between 0.02 mg/L for gentisic acid to 2 mg/L for resveratrol.

The fluorescent properties of assayed fluorophores are summarized in **Table 2**, together with four PARAFAC components, in the form of maximum excitation and emission wavelengths. Excitation and emission spectra for these candidates are presented in **Figure 5**. It can be deduced from these measurements that catechin and epicatechin wavelengths match well with those of PARAFAC component 2. *p*-Coumaric acid, *trans*-resveratrol, *trans*-piceid, and gentisic acid fluorescent properties are close to PARAFAC component 3. Lastly, vanillic acid could be related to PARAFAC component 4, because of the proximity of emission spectra and various maxima in the excitation one. Except for catechin and epicatechin, no exact match with the PARAFAC loadings was found, which supports the idea that each PARAFAC component does not necessarily correspond to a single fluorescent molecule, but more probably to a conglomerate or family of fluorescent molecules of related behavior.

HPLC Analysis of Wine Samples. Three chromatograms corresponding to the same wine sample, monitoring the eluate at the three different wavelengths pairs $\lambda_{exc/em}$ 260/360 (compromising wavelengths for PARAFAC components 1 and 4), 275/320 (PARAFAC component 2), and 330/410 nm (PARAFAC component 3), are shown in **Figure 6**. The global fluorescence intensity with excitation at 330 nm is quite small compared to those obtained for excitation at 260 nm or even at 275 nm.

Once the chromatograms had been registered for all samples, possible correlations between PARAFAC scores and the heights

of peaks corresponding to single compounds found in the chromatograms at the respective excitation and emission wavelengths were searched for.

For the first PARAFAC component, high correlations were found between its scores and the heights of peaks at 34.5 and 30 min in the FLD profiles at $\lambda_{exc/em}$ 260/360 nm ($R = 0.8236$ and 0.8261, respectively) (**Figure 7A**). The emission spectra ($\lambda_{exc} = 260$ nm) in the apex of these peaks were online registered. It was found that the emission spectrum of the compound eluting at 34.5 min was very similar to the emission profile corresponding to the first PARAFAC component. The molecular weight of this compound was deduced by LC-MS, resulting to be 534, a very high value, suggesting a condensation compound, probably a dimer. The emission spectrum for the compound eluting at 30 min was located in the same wavelength region as the emission profile of PARAFAC component 1, but the shape of this band differed notably. By spiking assays, it was deduced that these peaks (30 and 34.5 min) did not correspond to any of the assayed standards.

Not very good correlation was found between the scores of PARAFAC component 4 and the height of the peak corresponding to vanillic acid (retention time = 25 min) measured on the set of chromatograms at $\lambda_{exc/em}$ 260/360 nm, which suggests that vanillic acid alone is not responsible for this component but might be part of a group of molecules of similar fluorescent behavior.

The highest correlations were found between the score values of the second PARAFAC component and the heights of the peaks corresponding to catechin ($R = 0.9221$) and epicatechin ($R = 0.8761$) (retention time = 22.2 and 27.7 min, respectively), measured in the set of chromatograms obtained at $\lambda_{exc/em} = 275/320$ nm (**Figure 7B**). This supports the above assumption that these compounds are responsible for component 2. This fact is highly attractive because a rapid fluorometric measurement of these compounds would be valuable.

The third PARAFAC component scores correlated fairly well with some of the peaks in the chromatograms obtained at $\lambda_{exc/em}$ 330/410 nm, namely, peaks at 28.7, 30.2 (*p*-coumaric acid), 33, and 36.3 min.

To sum up, the potential of fluorescence excitation emission matrices as fingerprints of red wine samples has been demonstrated. PARAFAC decomposition has proven to be a useful tool for analyzing and interpreting this kind of complex data. Certain identification of the four detected fluorescent components was not fully achieved; however, a better knowledge of the fluorescent properties of red wines has been established and will serve as a basis for further studies. Certain identification of all the detected PARAFAC components should be one of the main future challenges. Catechin and epicatechin are probably the origin for one of the PARAFAC components and can be exploited for rapid fluorometric quantification.

The fluorescence spectra contain information about the quality and origin of the wines, and the methodology could be evaluated for certain authenticity and quality issues relevant to red wine.

ACKNOWLEDGMENT

We thank Arcus AS (Oslo, Norway) for supplying the carefully selected set of red wines.

LITERATURE CITED

(1) Christensen, J.; Norgaard, L.; Bro, R.; Engelsen, S. B. Multivariate autofluorescence of intact food systems. *Chem. Rev.* **2006**, *106*, 1979–1994.

(2) Strasburg, G. M.; Ludescher, R. D. Theory and applications of fluorescence spectroscopy in food research. *Trends Food Sci. Technol.* **1995**, *6*, 69–75.

(3) Dufour, É.; Letort, A.; Laguet, A.; Lebecque, A.; Serra, J. N. Investigation of variety, typicality and vintage of French and German wines using front-face fluorescence spectroscopy. *Anal. Chim. Acta* **2006**, *563*, 292–299.

(4) Wold, J. P.; Mielnik, M.; Pettersen, M. K.; Aaby, K.; Baardseth, P. Rapid assessment of rancidity in complex meat products by front face fluorescence spectroscopy. *J. Food Sci.* **2002**, *67*, 2397–2404.

(5) Andersen, C. M.; Wold, J. P. Fluorescence of muscle and connective tissue from cod and salmon. *J. Agric. Food Chem.* **2003**, *51*, 470–476.

(6) Wold, J. P.; Veberg, A.; Nilsen, A.; Iani, V.; Jucenas, P.; Moan, J. The role of naturally occurring chlorophyll and porphyrins in light-induced oxidation of dairy products. A study based on fluorescence spectroscopy and sensory analysis. *Int. Dairy J.* **2005**, *15*, 343–353.

(7) Kissmeyer-Nielsen, A.; Jensen, S. A.; Munck, L. The botanical composition of rye and rye milling fractions determined by fluorescence spectrometry and amino-acid composition. *J. Cereal Sci.* **1985**, *3*, 181–192.

(8) Seiden, P.; Bro, R.; Poll, L.; Munck, L. Exploring fluorescence spectra of apple juice and their connection to quality parameters by chemometrics. *J. Agric. Food Chem.* **1996**, *44*, 3202–3205.

(9) Ruoff, K.; Karoui, R.; Dufour, E.; Luginbuhl, W.; Bosset, J. O.; Bogdanov, S.; Amado, R. Authentication of the botanical origin of honey by front-face fluorescence spectroscopy. A preliminary study. *J. Agric. Food Chem.* **2005**, *53*, 1343–1347.

(10) Bro, R. PARAFAC. Tutorial and applications. *Chemom. Intell. Lab. Syst.* **1997**, *38*, 149–171.

(11) Andersen, C. M.; Bro, R. Practical aspects of PARAFAC modelling of excitation−emission data. *J. Chemom.* **2003**, *17*, 200–215.

(12) Bro, R. Exploratory study of sugar production using fluorescence spectroscopy and multi-way analysis. *Chemom. Intell. Lab. Syst.* **1999**, *46*, 133–147.

(13) Moller, J. K. S.; Parolari, G.; Gabba, L.; Christensen, J.; Skibsted, L. H. Monitoring chemical changes of dry-cured Parma ham during processing by surface autofluorescence spectroscopy. *J. Agric. Food Chem.* **2003**, *51*, 1224–1230.

(14) Pedersen, D. K.; Munck, L.; Engelsen, S. B. Screening for dioxin contamination in fish oil by PARAFAC and N-PLSR analysis of fluorescence landscapes. *J. Chemom.* **2002**, *16*, 451–460.

(15) Christensen, J.; Becker, E. M.; Frederiksen, C. S. Fluorescence spectroscopy and PARAFAC in the analysis of yogurt. *Chemom. Intell. Lab. Syst.* **2005**, *75*, 201–208.

(16) Christensen, J.; Povlsen, V. T.; Sorensen, J. Application of fluorescence spectroscopy and chemometrics in the evaluation of processed cheese during storage. *J. Dairy Sci.* **2003**, *86*, 1101–1107.

(17) Sikorska, E.; Romaniuk, A.; Khmelinskii, I. V.; Herance, R.; Bourdelande, J. L.; Sikorski, M.; Koziol, J. Characterization of edible oils using total luminescence spectroscopy. *J. Fluoresc.* **2004**, *14*, 25–35.

(18) Guimet, F.; Ferre, J.; Boque, R.; Rius, F. X. Application of unfold principal component analysis and parallel factor analysis to the exploratory analysis of olive oils by means of excitation−emission matrix fluorescence spectroscopy. *Anal. Chim. Acta* **2004**, *515*, 75–85.

(19) Rinnan, Å.; Andersen, C. M. Handling of first-order Rayleigh scatter in PARAFAC modelling of fluorescence excitation−emission data. *Chemom. Intell. Lab. Syst.* **2005**, *76*, 91–99.

(20) Ewing, G. W. *Instrumental Methods of Chemical Analysis*; McGraw-Hill: New York, 1985.

(21) Leurgans, S.; Ross, R. T. Multilinear models: applications in spectroscopy (with discussion). *Stat. Sci*. **1992**, *7*, 289–319.
(22) Unscrambler v. 6.11b, CAMO A/S, Trondheim, Norway.
(23) Harshman, R. A.; de Sarbo, W. S. An application of PARAFAC to a small sample problem, demonstrating preprocessing, orthogonality constraints, and split-half diagnostic techniques. In *Research Methods for Multimode Data Analysis*; Law, H. G., Snyder, C. W., Hattie, J. A., McDonald, R. P., Eds.; Praeger: New York, 1984; pp 602−642.
(24) Burns, J.; Gardner, P. T.; Matthews, D.; Duthie, G. G.; Lean, M. E. J.; Crozier, A. Extraction of phenolics and changes in antioxidant activity of red wines during vinification. *J. Agric. Food Chem*. **2001**, *49*, 5797–5808.

Received for review July 1, 2008. Revised manuscript received January 13, 2009. Accepted January 14, 2009. We are grateful to Junta de Extremadura for Project PRI08A049. D.A.-R. is grateful to Consejería de Infraestructura y Desarrollo Tecnológico, Junta de Extremadura, for a fellowship (DOE 22/06/04).

JF8033623